

UNCLASSIFIED

AD 285 582

*Reproduced
by the*

**ARMED SERVICES TECHNICAL INFORMATION AGENCY
ARLINGTON HALL STATION
ARLINGTON 12, VIRGINIA**



UNCLASSIFIED

NOTICE: When government or other drawings, specifications or other data are used for any purpose other than in connection with a definitely related government procurement operation, the U. S. Government thereby incurs no responsibility, nor any obligation whatsoever; and the fact that the Government may have formulated, furnished, or in any way supplied the said drawings, specifications, or other data is not to be regarded by implication or otherwise as in any manner licensing the holder or any other person or corporation, or conveying any rights or permission to manufacture, use or sell any patented invention that may in any way be related thereto.

285 582

AF CRL-62-859

Final Report

AN EXAMINATION OF SOME TIROS II RADIATION DATA AND RELATED STUDIES

Prepared for:

GEOPHYSICS RESEARCH DIRECTORATE
AIR FORCE CAMBRIDGE RESEARCH LABORATORIES
OFFICE OF AEROSPACE RESEARCH
UNITED STATES AIR FORCE
BEDFORD, MASSACHUSETTS

CONTRACT AF 19(628)-3
PROJECT 6698
TASK 66982

By: P. M. Lunkawa, P. A. D. L., W. A. L.

UNCLASSIFIED
AS AD NO.

SECRET
OCT 12 1962
RECEIVED
TISA

Best Available Copy

Requests for additional copies by Agencies of the Department of Defense, their contractors, and other Government agencies should be directed to the:

ARMED SERVICES TECHNICAL INFORMATION AGENCY
ARLINGTON HALL STATION
ARLINGTON 12, VIRGINIA

Department of Defense contractors must be established for ASTIA services or have their "need-to-know" certified by the cognizant military agency of their project or contract.

All other persons and organizations should apply to the:

U.S. DEPARTMENT OF COMMERCE
OFFICE OF TECHNICAL SERVICES
WASHINGTON 25, D.C.

STANFORD RESEARCH INSTITUTE

MENLO PARK, CALIFORNIA



July 1962

AF CRL-62-859

Final Report

AN EXAMINATION OF SOME TIROS II RADIATION DATA AND RELATED STUDIES

Prepared for:

GEOPHYSICS RESEARCH DIRECTORATE
AIR FORCE CAMBRIDGE RESEARCH LABORATORIES
OFFICE OF AEROSPACE RESEARCH
UNITED STATES AIR FORCE
BEDFORD, MASSACHUSETTS

CONTRACT AF 19(628)-322
PROJECT 6698
TASK 66982

By: P. M. Furukawa P. A. Davis W. Viezee

SRI Project No. 3989

Approved:

M. G. H. LIGDA, MANAGER AEROPHYSICS LABORATORY

D. R. SCHEUCH, DIRECTOR ELECTRONICS AND RADIO SCIENCES DIVISION

Copy No. 48

ABSTRACT

Sample radiation maps selected from the Tiros II Radiation Data Catalog, Vol. 1, are examined in order to evaluate their representativeness and limitations. The difficulties encountered in the examination of the data for Channel 1 (6.0 to 6.5 μ) are described. The averaged catalog data for Channel 2 (8 to 12 μ) are compared with the synoptic situation, the actual measurements, and the calculated values of the intensity in the zenith direction. A general discussion of the radiative budget of the troposphere and its relationship to the upward flux at the tropopause is also presented.

CONTENTS

ABSTRACT.	11
LIST OF ILLUSTRATIONS	iv
LIST OF TABLES.	iv
I INTRODUCTION	1
II THE EXAMINATION AND EVALUATION OF SOME TIROS II RADIATION DATA	2
A. General	2
B. Discussions of Channel 1 (6.0 to 6.5 μ).	3
C. Discussions of Channel 2 (8 to 12 μ)	4
1. Comparison of Tiros II Data with a Nephanalysis	4
2. Comparison of the Averaged and Actual Tiros II Data.	10
3. Comparison of Tiros II Radiation Data with Computed Upward Intensities.	13
III COMMENTS ON THE TROPOSPHERIC RADIATIVE BUDGET FOR OMAHA, NEBRASKA, 12-18 MARCH 1957.	18
A. Local Variations of the Tropospheric Radiative Budget.	18
B. Average Energy Loss vs. Energy Loss for Averaged Conditions.	20
REFERENCES.	24

ILLUSTRATIONS

Fig. 1	Comparison of Averaged and Actual Tiros II Radiation Data--Channel 1 (6.0 to 6.5μ), Orbit 74, 28 November 1960.	5
Fig. 2	Comparison of Tiros II Radiation Map vs. Synoptic Cloud Distributions--Channel 2 (8 to 12μ), Orbit 74, 28 November 1960.	6
Fig. 3	Comparison of Averaged and Actual Tiros II Radiation Data--Channel 2 (8 to 12μ), Orbit 74, 28 November 1960.	12
Fig. 4(a)	Comparison of Averaged Tiros II Radiation Data vs. Computed Intensities--Channel 2 (8 to 12μ), Orbit 74, 28 November 1960.	16
Fig. 4(b)	Atmospheric Cross Section Along Sub-Satellite Path, 1200Z, 28 November 1960	16

TABLES

Table I	Tropospheric Outgoing Long-Wave Flux (F_0) vs. Total Net Radiative Cooling (ΔE_T), 12-16 March 1957, Omaha, Nebraska	20
Table II	Actual and Estimated Average Radiative Cooling Rates in the Troposphere, 12-16 March 1957, Omaha, Nebraska	22

AN EXAMINATION OF SOME TIROS II RADIATION DATA AND RELATED STUDIES

I INTRODUCTION

In an earlier study^{1*} of the present project, semi-theoretical methods were employed to calculate the vertically directed upward intensities of radiation at the top of the atmosphere and the contributions to these intensities by the atmosphere, earth, and clouds. The purpose of the study was to illustrate the variations in the upward intensities resulting from different meteorological conditions existing in the atmosphere. The calculations, covering a period of varying weather at Omaha, Nebraska, were made for spectral intervals of 6.0 to 6.5 μ and 8 to 12 μ . These intervals closely correspond to the bandwidths of Channels 1 and 2, respectively, of the Tiros II medium-resolution radiometer. A full discussion of the methods used in the calculations and the analyses of the results was presented in Scientific Report No. 1 under the current contract.

The tasks which were accomplished during the later phases of the project are described in this Final Report. The discussions are presented in two parts. The first (Sec. II) is concerned with the examination and evaluation of some sample Tiros II radiation measurements. The second part (Sec. III) consists of a general discussion of the tropospheric radiative heat budget and its relationship with the upward flux at the tropopause.

*References are listed at the end of this report.

II THE EXAMINATION AND EVALUATION OF SOME TIROS II RADIATION DATA

A. General

A problem posed by the large quantity of data provided by the Tiros II radiation experiments is that of finding a convenient form for the presentation and use of the data. The normal course of action would be to average the numerous measurements by techniques or methods that might be dictated by the use intended for the data. One such presentation is the series of radiation maps in the Tiros II Radiation Data Catalog, Vol. I, which was prepared by the staff members of the Aeronomy and Meteorology Division, Goddard Space Flight Center, NASA, and the Meteorological Satellite Laboratory, USWB. The averaged radiation data in the catalog are presented in two map forms. One is a low-resolution map based on large amounts of data (about 50-minutes time span) averaged at grid points on a hemispheric polar stereographic base. The other is a high-resolution map on which data for about a five-minute time span are fitted to a finer mesh grid by use of a revised JNWP objective analysis technique.

In an effort to evaluate the limitations and representativeness of averaged quantilics in an interpretative application, samples of the radiation maps presented in the catalog were examined. The averaged catalog data were used since, apart from the bulk of the original data, they represent the only source of satellite radiation measurements that, at the present time, are readily available in a form convenient for wide use. Because of the limited nature of the project, no extensive interpretive study of the data was attempted and measurements of only two of the five channels of the Tiros II radiometer were considered.

The selection of the data for the study was based on the following considerations: (1) measurements should be for the continental U.S. where supporting meteorological data are relatively dense and easily obtained; (2) satellite observations should be near the observation times of the meteorological data; and (3) the synoptic weather situation should

be such that various degrees of cloud cover were present. These requirements were well met by the data selected for the study--namely, the data from a portion of Orbit 74 on 28 November 1960.

B. Discussions of Channel 1 (6.0 to 6.5 μ)

The results of the examination of data from Channel 1 proved to be rather disappointing. Without further study beyond the scope intended for the present evaluation, no conclusive results were obtained. However, it may be of interest to note the factors leading to the difficulties encountered in the study of the Channel 1 data.

- (1) Perhaps the most significant factor was the small amount of energy that is accepted by the sensors of Channel 1. In addition, these amounts vary only slightly in absolute magnitude for a wide range of meteorological conditions in the atmosphere. The result is that it is difficult to establish any consistent relationship between the distribution of the measured radiation values and the synoptic situation.
- (2) Wark² has shown that the effects of limb darkening were greater for Channel 1 than for Channel 2. However, limb darkening effects did not account for some of the inconsistencies in the distribution of the observed radiation values.
- (3) The large part of the total radiant energy measured within the spectral limits of Channel 1 is due to the upward emission by the water vapor in the atmosphere. Thus for proper interpretation of the Channel 1 data, it is necessary to have information on the distribution of atmospheric moisture. In the present case, such information was generally inadequate for levels higher than 400 mb.

(4) Although the magnitudes of the measured radiation in both the tabulated listing of the original data and the averaged radiation map appear reasonable, there is some uncertainty in the representativeness of differences between the discrete values (0.25, 0.37, 0.50, etc. watts/meter²) adopted in the tabulation. Furthermore, the averaged values presented in the radiation map show no variations in the intervals between isopleths, which means that the values increase or decrease (albeit in small amounts) in "steps" at the isopleths. The reliability and significance both of the absolute magnitudes presented in the tabulations, and of the variations, as shown by the mapped patterns of the averaged radiation, are difficult to assess. Obviously, the low amounts of measured energy contribute to this problem.*

(5) A comparison (see Fig. 1) of the averaged and actual measurements for Channel 1 showed that the magnitudes of the actual data were not well represented by the averaged values and while some of the variations of both sets of data were in phase, others were not. These results are again manifestations of the small amounts of energy being measured in Channel 1.

C. Discussions of Channel 2 (8 to 12μ)

1. Comparison of Tiros II Data with a Nephanalysis

A high-resolution radiation map for Channel 2, Orbit 74, from the Tiros II radiation Data Catalog is shown in Fig. 2. The map represents measurements taken over the western half of the U.S. during the

* Some difficulties were encountered in the initial data processing due to low signal-to-noise ratio (F. R. Valovcin, private communication).

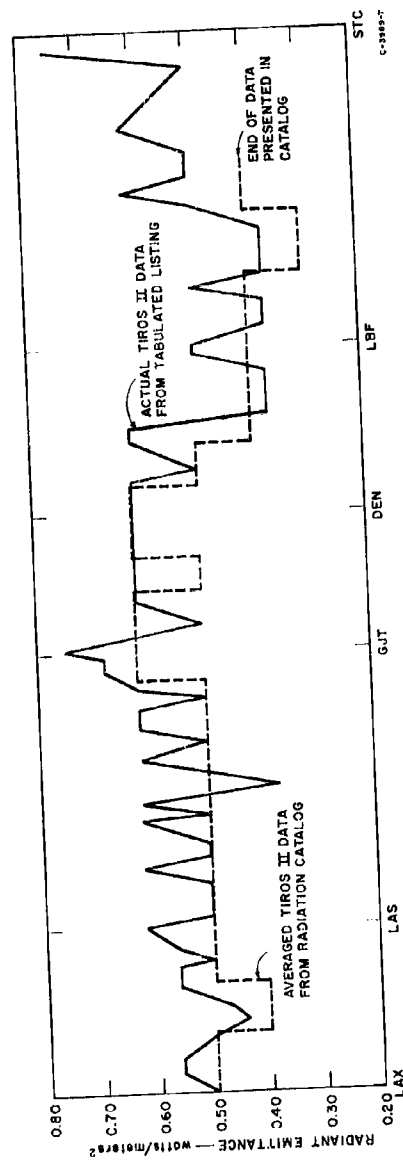


FIG. 1 COMPARISON OF AVERAGED AND ACTUAL TIROS II RADIATION DATA -
CHANNEL 1 (6.0 to 6.5 μ), ORBIT 74, 28 NOVEMBER 1960

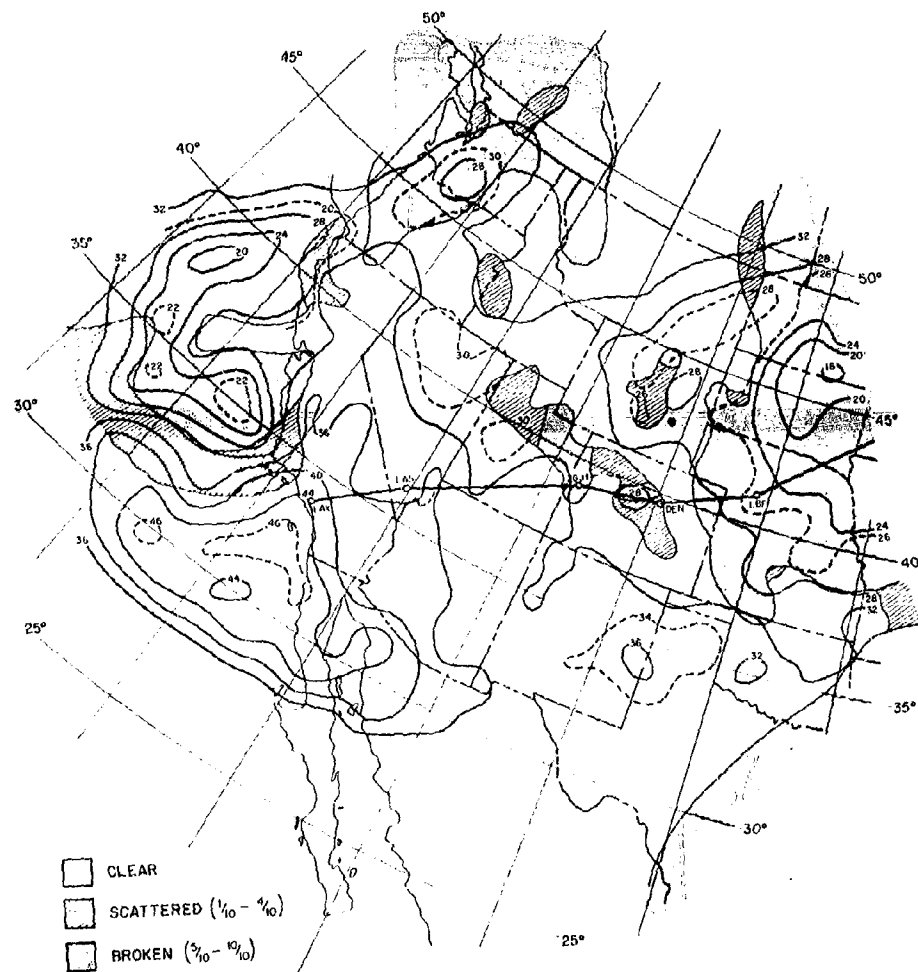


FIG. 2 COMPARISON OF TIROS II RADIATION MAP vs. SYNOPTIC CLOUD DISTRIBUTIONS - CHANNEL 2 (8 to 12 μ), ORBIT 74, 28 NOVEMBER 1960
Units: watts/meter²
Source: Tiros II Radiation Data Catalog, NASA and USWB

period from about 1210Z to 1218Z, 28 November 1960. Superimposed on the radiation map is an analysis of the synoptic cloud distribution for 1200Z on the same day. The cloud data for the analysis were obtained from the surface synoptic data presented in the U.S. Weather Bureau's Northern Hemisphere Data Tabulations. These were further supplemented by the cloud information contained in WBAN 10 A's and B's for the stations not listed in the Data Tabulations. In making the analysis, the reported cloud amounts were arbitrarily divided into three classifications and represented in Fig. 2 as: clear (unshaded area), no clouds; scattered (hatched area), one- to four-tenths cloud cover; and broken (shaded area), five-tenths-to-overcast cloud cover.

Earlier comparisons^{3,4,5,6} of Tiros II and III radiation data with nephanalysis have already shown the relatively good correlation between the distribution patterns of the measured radiation for Channel 2 and the large-scale cloud distributions. The comparison in Fig. 2 is presented in order to point out other interesting features of this particular case and to indicate some areas which seem to warrant further investigation.

As in the other studies, the large-scale cloud distribution in Fig. 2 compares remarkably well with the distribution patterns of the averaged radiation values. In general, the low radiation values encompass the areas of broken-to-overcast cloud cover, the higher values encompass the clear areas, and areas of scattered cloudiness coincide with the transitional area between the high and low values of measured radiation.

Fritz and Winston³ found that over a broad area, low radiation values represented by the isotherm for an equivalent black-body temperature of 250°K generally encompassed most of the rain area. In the present case, this was true over North and South Dakota and Nebraska where the stations in the area enclosed by the "26" isopleth reported continuous snowfall at map time. The heaviest snowfall was reported at Huron, South Dakota, just to the south of the center of the lowest values.

Over the Pacific Ocean, however, only two of the thirteen ships in the cloud area from 30°N to 40°N reported any precipitation and, in both cases, it was of the convective type (showers). The reported cloud types for the area were thick and thin As, Sc, and Cu. No precipitation was reported by the stations in the broken-to-overcast cloud-cover area in Oregon and Washington, but both high (Cs) and dense middle clouds (double-layered or thick Ac or Ac with As and/or Ns) were generally reported by the stations in the area.

A point of interest is the area of clear skies extending in a southwesterly direction from the California coast just to the north of the San Francisco Bay region and a similar area of a northwest-southeast direction at the California-Oregon border. In the initial cloud analysis based on only the published surface reports and independent of the radiation map, the broken-to-overcast cloud area was drawn so that its border extended down the middle of Washington, Oregon, and California to about 35°N and then out over the ocean. Supplementary WBAN 10 A and B cloud data then suggested the clear and scattered cloud areas included in Fig. 2. In the final analysis, the boundaries of the clear areas were suggested by the distribution patterns of the radiation values and were drawn as shown in Fig. 2. It might be noted that Farallone Island, which is just outside of the entrance to San Francisco Bay, and a ship at 37°N, 126.5°W reported "clear" and "one-tenth or less" cloudiness, respectively.

The following comments are pertinent to the present discussions:

- (1) Although the cloud cover has been analyzed without violating any of the reported synoptic data and is consistent with the patterns of radiation values, the analysis still needs confirmation by some other method such as satellite cloud pictures or good albedo measurements. Unfortunately, no pictures were available for the case being presented and the study of albedo measurements was not a part of the present work.

(2) If the cloud analysis as presented in Fig. 2 is correct, then it would appear that additional studies along the same line should be made in an endeavor to establish some criteria by which a nephanalysis might be made from the radiation maps. If this can be accomplished, the radiation data would be useful for determining nighttime and "silent area" cloud cover and, in absence of pictures, for making a more detailed cloud analysis than perhaps can be done from the reported synoptic data.

(3) An example of the type of criteria that might be established from additional studies is the relationship between the areas of precipitation and the area enclosed by particular isopleths on radiation maps. It is interesting to note that not all cloud areas enclosed by the "26" isopleth in Fig. 2 reported precipitation. On the other hand, the precipitation areas coincident with the "25-26" isopleth in both this study and that of Fritz and Winston³ were located over relatively low and flat terrain on the eastern side of mountain ranges (i.e., the Rocky Mountains and the Appalachian-Blue Ridge Mountains).

The relationship between the radiation patterns and the cloud distributions in the Rocky Mountain states is more difficult to interpret because of the effects of the high mountain ranges. For instance, one is tempted to assign the low radiation values just to the west of Denver (DEN) to the broken-to-overcast cloud cover. However, the cloud analysis is based on one station (Fraser) reporting eight-tenths cloud cover, and it would be difficult to say whether the low radiation values were due to the clouds or the presence of the high mountains in the area.

In the clear-sky area, most of the radiant energy measured in Channel 2 is from the ground surface and therefore should be related to the radiation temperature of the surface. No evaluation of a relationship could be made because of the lack of pertinent surface data. However, Fritz and Winston found that the equivalent black-body temperatures of the measured radiation were close to the air temperatures measured in the shelter under cloudless conditions. While no direct comparison between equivalent temperatures and the reported screen-height air temperatures were made in the present study, some parallels were found between their distribution in the cloudless areas. For example, starting with the high radiation values off the coast of Southern California and going eastward along the 34°N latitude circle, the following surface air temperatures were reported: 56° to 63°F over the ocean, 45° to 47°F at the coastal stations, 31° to 37°F along central and southern parts of Arizona and New Mexico, and 37° to 40°F in the area of the high radiation values in eastern New Mexico and Texas. A look at the distribution of the radiation values along the same line shows the highest values over the ocean, decreasing eastward to the coast where a relatively sharp decrease occurs, then a continual but more gradual decrease to about the Arizona-New Mexico border, from which there is an increase to the high values in eastern New Mexico and Texas.

Other areas that show similar relationships are in northern Nevada where the "dashed 30" isopleth covers the area with stations reporting temperatures of 8° to 15°F and in southeast Montana where temperatures of 2° to 7°F were reported by the stations within the "dashed 26" isopleth. Likewise, the "loughs" in southern Utah and Colorado must reflect the colder temperatures of mountain ranges--in this case, the Wasatch Mountains in Utah, and the Sangre de Cristo and San Juan ranges in Colorado and New Mexico.

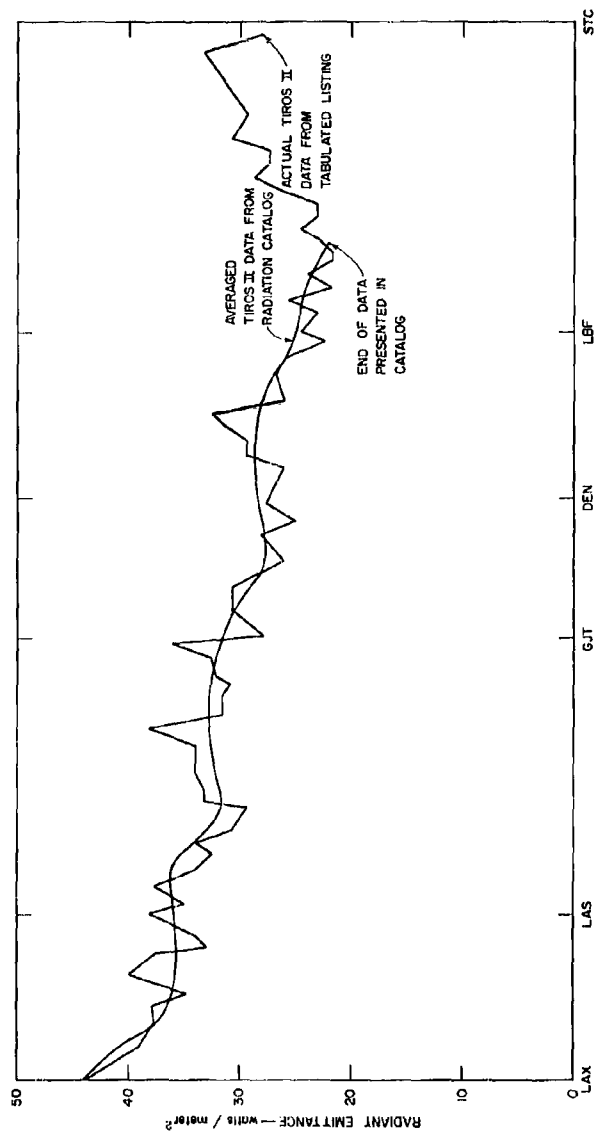
2. Comparison of the Averaged and Actual Tiros II Data

A comparison of the averaged and actual data was made in order to see how well the averaged data represented the actual measurements, and to determine the degree of "smoothing" resulting from the particular

averaging technique used in the data catalog. Data taken from along the track designated in Fig. 2--i.e., LAX-LAS-GJT-DEN-LBF--was used for the purposes of the comparison. The reasons for this selection are: (1) the track runs very closely to the sub-satellite path of Orbit 74, thus involving data of minimum nadir angle; (2) a cross-section, which is discussed in the next section, was drawn along the designated line; (3) the synoptic conditions along the track ranged from clear skies to overcast; and finally (4) a plot of the original data showed the locations of the viewed points to be most reliable near the sub-satellite path.

The averaged and actual values along the track were determined independently. The averaged values were obtained directly from the radiation map presented in the data catalog. The actual data were first plotted on a map from a tabulated listing. When the plotted values were within about 25 to 30 miles of the track, they were used directly. At distances greater than 25 to 30 miles from the track, two readings (one on each side of the track) of a given sweep were averaged and the mean was assumed to be valid at the sub-satellite point. The two resulting curves, one representing the averaged data, the other the actual, are shown in Fig. 3. An idea of the distance between successive viewing sweeps of the radiometer may be obtained from the horizontal distance between the individual "points" on the curve of the actual data. The average horizontal distance between "points" was found to be about 20 miles.

An examination of the curves in Fig. 3 shows that the average curve fits the actual curve very well. Judging from the curves, it appears that the averaged values generally are representative of areas of no less than about 100, or perhaps 150, miles square. There is some suggestion by the curve presented in Fig. 3 that some of the oscillation smoothed over by the averaging technique used in the data catalog may be significant. For example, at Denver (DEN), it would not be unreasonable to interpret the lower values represented by the "trough" of the actual curve as the resultant radiation of the higher mountains. The following



RC-3989-S

FIG. 3 COMPARISON OF AVERAGED AND ACTUAL TIROS II RADIATION DATA -
CHANNEL 2 (8 to 12 μ), ORBIT 74, 28 NOVEMBER 1960

peak (between DEN and LBF) of the actual curve agrees favorably with the clear skies in the area (see Fig. 2) and the warmer radiating temperatures of the lower plains. Further east, the lower radiation values can then be attributed to the overcast cloud cover near LBF. The general trend is indicated by the average curve, but it does not contain enough detail to make the analysis as described. The determination of the scale of the significant oscillations of the radiation data, especially in terms of synoptic features, is an area that needs further study.

It is conceivable that the individual values of the actual data may well represent the real fluctuations resulting from, say, a cold mountain peak and a warmer neighboring valley. However, the utility of detailed individual values is doubtful because of other uncertainties, such as the location of the viewed area. In addition, it would be difficult to confirm such small-scale interpretations with the general synoptic data presently available.

3. Comparison of Tiros II Radiation Data with Computed Upward Intensities

In this section, the measured radiation values are compared with the calculations of the vertically directed upward intensities at the top of the atmosphere. The methods of calculation were discussed in detail in Scientific Report 1¹ and will be reviewed here only briefly.

The total upward intensity, I_T , of a spectral band emerging from the top of the atmosphere under clear sky conditions may be expressed as

$$I_T = \sum_{p=p_0}^{p=10} I_{\Delta p} + \int_{\Delta\lambda} [B_{\lambda}(T_s) \tau_s(\lambda)] d\lambda \quad (1)$$

where $I_{\Delta p}$ is the contribution by each atmospheric layer of thickness Δp to the total intensity I_T , $B_\lambda(T_s)$ is the specific intensity of the black-body radiation at the temperature T_s of the earth's surface, and $\tau_s(\lambda)$ is the wavelength-dependent monochromatic transmissivity of the atmosphere from the earth's surface where $p = p_0$, to the assumed effective top of the atmosphere--i.e., where $p = 10$ mb. Under overcast conditions, the atmospheric contributions are summed from the level of the cloud tops to $p = 10$ mb, and the contribution from the earth's surface is replaced by the black-body radiation from the cloud top. In the case of partial cloudiness, I_T was determined for clear and overcast conditions and then weighted according to the amount of cloud cover present.

The calculations of I_T were made for the spectral interval, 8 to 12μ , which corresponds approximately to Channel 2 of the Tiros II radiometer. The total atmospheric transmissivity for the interval was assumed to result from (1) weak line absorption in the interval 8 to 10μ by the neighboring 6.3μ vibration-rotation band, and (2) continuous absorption throughout the 8-to- 12μ interval by the "wings" of the very strong lines at the peaks of the 6.3μ band and the rotational band. The weak line transmissivities were determined from the experimental results of Howard, Burch, and Williams.⁷ The transmissivities resulting from the continuous absorption were evaluated from the absorption coefficients given by Elsasser.¹¹

The meteorological data for the calculations were taken from the U.S. Weather Bureau's Northern Hemisphere Data Tabulation. The lack of data on the moisture content of the upper tropospheric levels and the stratosphere necessitated an extrapolation of all the mixing ratio soundings from 400 to 200 mb. This was accomplished by first plotting the available mixing ratio values for 500, 450, and 400 mb on a semi-log graph, and then fitting a smooth curve such that the curve terminated at 200 mb with a value of 0.008 g/kg. A model distribution of the stratospheric water vapor, which was adopted for use in the earlier study, was also used here for the region from 200 to 10 mb.

A cross section of the meteorological conditions along the track shown in Fig. 2 (LAX-LAS-GJT-DEN-LBF-STC) is presented in Fig. 4(b). As mentioned earlier, the track closely parallels the sub-satellite path of Orbit 74 of Tiros II. Cloud data were obtained from the Data Tabulation and from WBAN 10 A's and B's. Good estimates of cloud-base heights were available from these sources, but the more important data on the height of cloud tops were completely lacking. Consequently, cloud-top heights were estimated on the basis of the meteorological soundings and the reported cloud types. The clouds and their amounts (N) are presented in schematic form in Fig. 4(b).

The results of the intensity calculations, which were made for the stations designated along the bottom of the cross section, are shown in Fig. 4(a). The averaged radiation measurements for the cross section, evaluated previously (see Fig. 3), are also included in Fig. 4(a). Both the measured and computed values have been normalized for comparison and are presented in terms of percentages of their mean values.

A comparison of Figs. 4(a) and (b) shows that the largest changes in the curve of the averaged catalog data occur when there is a significant change in the larger-scale synoptic features. This is illustrated in the area of clear skies between LAX (Los Angeles) and GJT (Grand Junction). Starting with LAX, the radiation values drop rather sharply over the colder areas (less radiation) of the coastal mountain ranges and the inland valleys. The next large decrease occurs at the edge of the higher and still colder mountain area between LAS (Las Vegas) and GJT. In between the relatively large drops, the curve is uniform over the smaller valleys and ridges of the mountain ranges. This again serves to illustrate the need to determine the scale to which the radiation measurements can be reliably applied.

The plot of the computed values of the vertically directed upward intensities in Fig. 4(a) fit the general trend of the averaged curve fairly well. Under clear-sky conditions, the total upward intensity I_T [see Eq. (1)] at the top of the atmosphere for the 8-to-12 μ

1

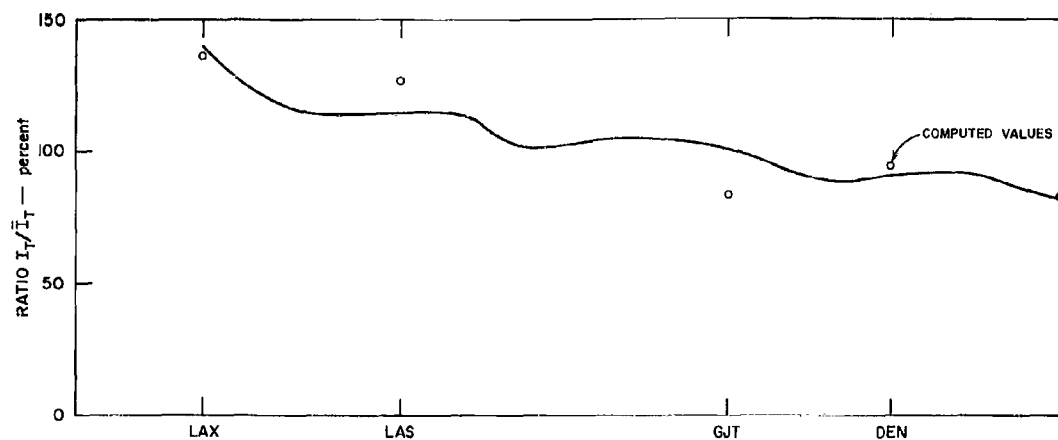


FIG. 4(a) COMPARISON OF AVERAGED TIROS II RADIATION DATA INTENSITIES - CHANNEL 2 (8 to 12 μ), ORBIT 74, 28 NOV

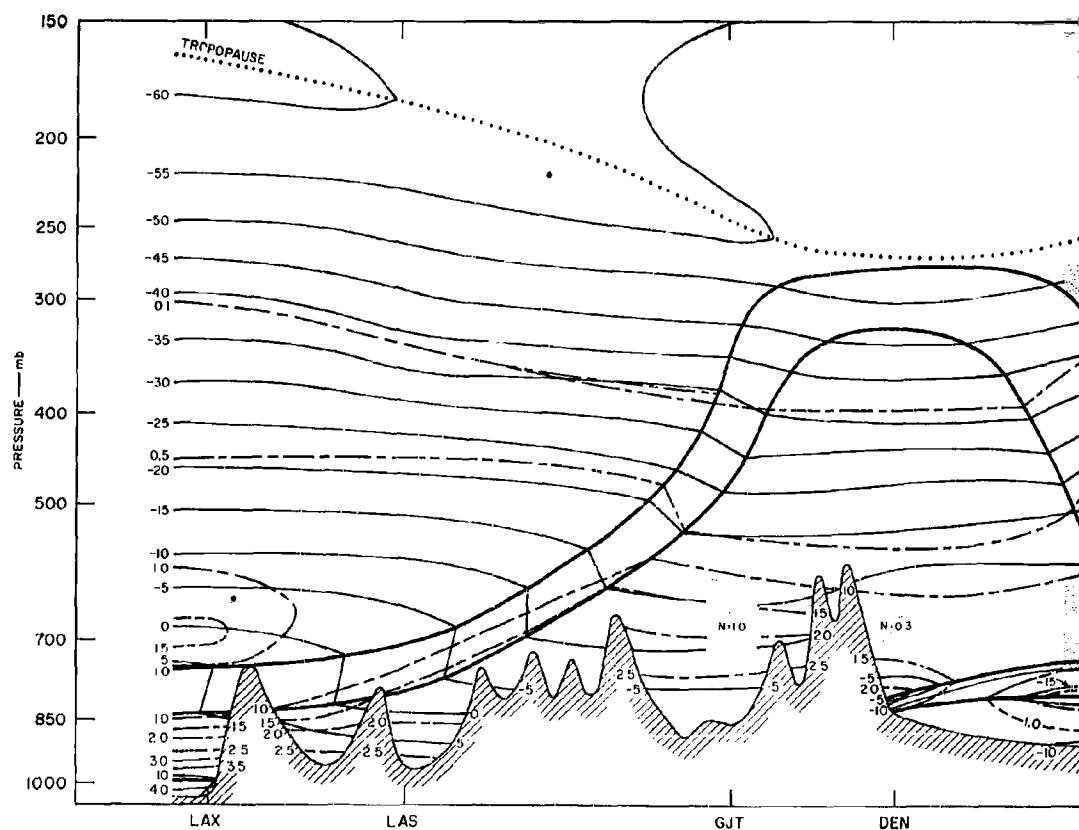


FIG. 4(b) ATMOSPHERIC CROSS SECTION ALONG SUB-SATELLITE 28 NOVEMBER 1960
Thin, solid lines are isotherms in $^{\circ}\text{C}$; dash-dot lines are isopneusts
Constant Mixing Ratio in g/kg; and heavy, solid lines represent

2

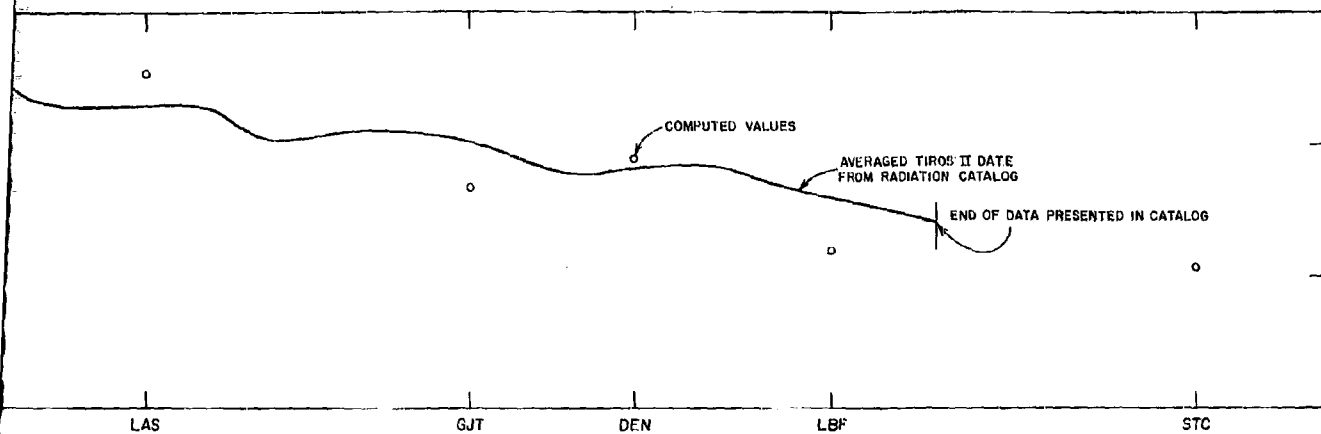


FIG. 4(a) COMPARISON OF AVERAGED TIROS II RADIATION DATA vs. COMPUTED INTENSITIES - CHANNEL 2 (8 to 12μ), ORBIT 74, 28 NOVEMBER 1960

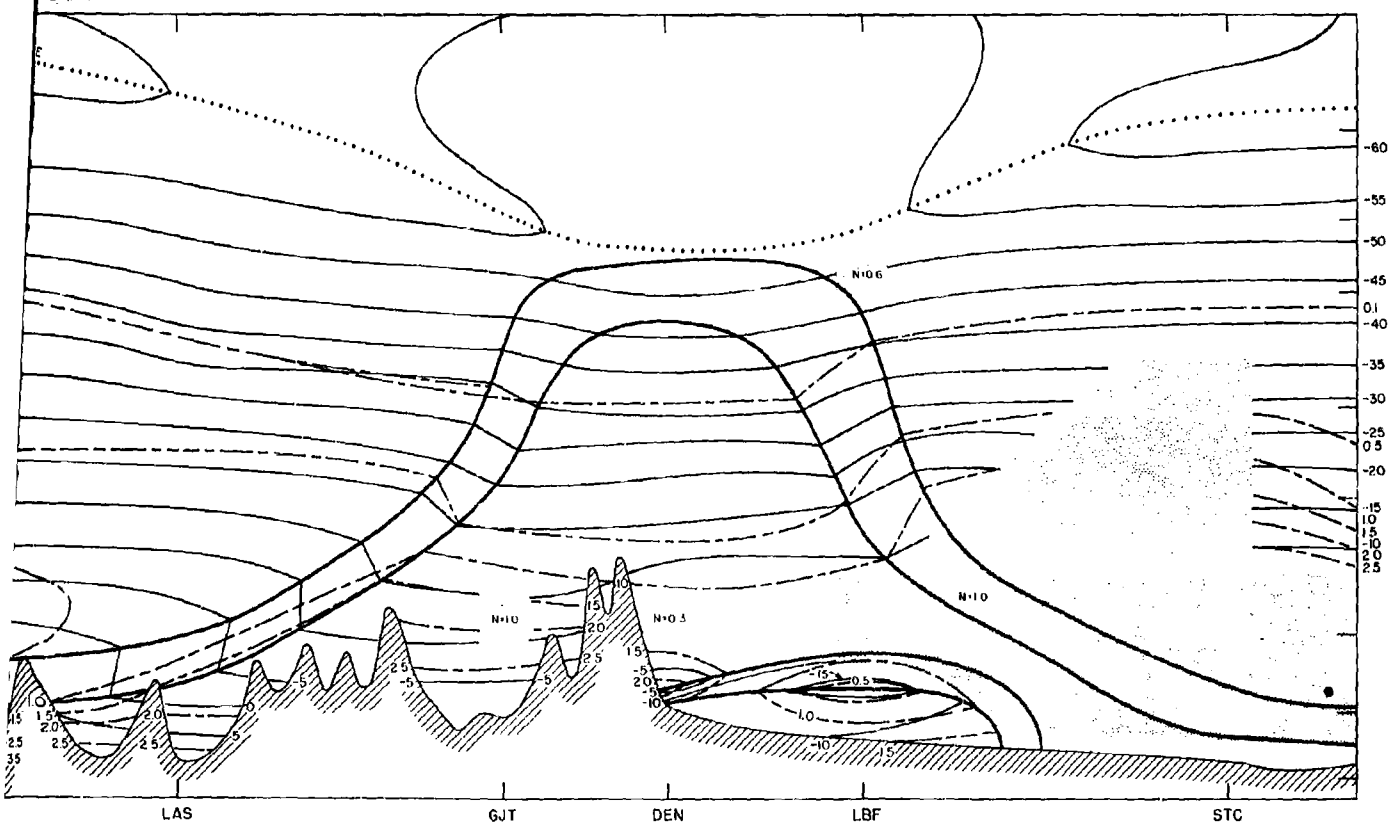


FIG. 4(b) ATMOSPHERIC CROSS SECTION ALONG SUB-SATELLITE PATH, 1200Z, 28 NOVEMBER 1960

Thin, solid lines are isotherms in $^{\circ}\text{C}$; dash-dot lines are isopleths of Constant Mixing Ratio in g/kg ; and heavy, solid lines represent fronts

band consists mostly of the transmitted black-body radiation from the earth's surface. Therefore it should give some indication of the earth's radiation temperature which, in the calculations, was assumed to be equivalent to the reported shelter-height air temperature. In the discussion of the previous section it was noted that the averaged radiation measurements in the clear sky also tended to reflect the trends in the distributions of the reported shelter temperatures. Thus it can be expected that under cloudless conditions, the computed and measured values will both show the same general trend. The same would be true for overcast conditions if the cloud layer(s) could be assumed to be black and if the effective radiation temperature could be estimated with sufficient accuracy.

It is interesting to note that the computed values for clear sky and partial cloudiness ($N = 0.3$) tend to be slightly closer but higher than the averaged measured values, whereas for overcast conditions all the computed values are lower. A discrepancy between the radiation data and the computed values is noted at STC (St. Cloud). The curve of the averaged data does not extend to the station, but the actual data curve in Fig. 3 indicates the trend to be increasing from LBF (North Platte) to STC, whereas the computed values show a decrease. The discrepancy probably results from an incorrect estimate of the cloud-top height in the calculations. The higher values of the actual radiation data indicate that the cloud tops were lower (warmer radiation temperatures) than assumed. This example underlines the need for adequate data on cloud-top heights for radiation studies.

III COMMENTS ON THE TROPOSPHERIC RADIATIVE BUDGET FOR OMAHA, NEBRASKA, 12-16 MARCH 1957

This section contains an evaluation of some properties of the tropospheric radiative budget that are of general interest for heat budget studies. The computations of the net long-wave flux divergences, based on the Elsasser chart, have been presented in a previous report.⁹ That report also outlines a procedure for computing the absorption of solar radiation by the troposphere for various conditions of cloudiness and surface albedo. Details of the solar calculations for Omaha have been described by Vizec.¹⁰ Since the conclusions concerning the radiative budget are based on a study at a single locality at one time of the year, their general applicability to all heat-budget studies must be viewed with reservation.

A. Local Variations of the Tropospheric Radiative Budget

With the exception of the surface layer, the tropospheric long-wave radiative cooling undergoes negligible diurnal variations. Significant variations in the radiative cooling are associated with changing sky conditions. During the period of the case study, below-average radiative cooling in the troposphere as a whole was associated with the high clouds, whereas above-average cooling occurred with the thick, low clouds. A smaller contribution to the variability arises from significant changes in the distribution of temperature and moisture.

The tropospheric solar heating follows a pronounced cycle from sunrise to sunset. Superposed on the diurnal variations due to a change in solar zenith angle are the effects of cloudiness. Reflective high clouds tend to reduce the total solar heating, whereas low, thick clouds can increase significantly the total solar heating, especially near local noon. Thus, the effect of clouds on the tropospheric solar heating is similar to the effect of clouds on the tropospheric long-wave cooling. In addition, variations of solar heating are induced by changes in moisture.

The long-wave cooling minus the solar heating yields the net radiative cooling. During nocturnal hours the tropospheric net radiative cooling is identical with the long-wave cooling, but during the day there is a pronounced reduction of the net cooling due to the absorption of short-wave solar radiation. Within the time period examined for Omaha, the maximum solar heating near local noon balanced the long-wave cooling on clear days and exceeded the long-wave cooling on cloudy days. However, for the total time period between sunrise and sunset a net cooling was evident. Over a complete 24-hour period with overcast skies, the net radiative cooling was only slightly larger than that during clear skies. This suggests that no serious underestimate of the average tropospheric cooling is made by neglecting clouds covering half or less of the sky. When only nocturnal periods are considered, the cloudiness is more significant to the total cooling.

The net radiative cooling in the troposphere is not directly deducible from a measure such as the upward long-wave flux leaving the troposphere, but for any particular time of day some relationship in the patterns of the two quantities might be anticipated. During daylight hours the net radiative cooling varies in proportion to the solar heating, while during the night the net cooling is steady and less responsive to synoptic changes than the outgoing flux. Both the outgoing flux and the net radiative cooling, taken from the Omaha study, are illustrated for two local times in Table I. At midafternoon on four consecutive days with both clear and cloudy skies the smallest outgoing long-wave flux was associated with the smallest tropospheric radiative cooling (actually a net heating). However, during clear skies at the same time of day the largest net cooling occurred in the drier air rather than in the air mass with the largest outgoing long-wave flux. For 2100 CST on four consecutive nights the largest outgoing long-wave flux was associated with the smallest tropospheric cooling, but no clear-cut relationship is obtained by grouping all four days together. The clearest relationship at both local times is demonstrated by separating the two clear days from the two overcast days. Then it is apparent that during

overcast conditions the smallest outgoing flux is associated with the smallest net cooling, while during clear skies, the smallest outgoing flux is associated with the largest net cooling.

Table I

TROPOSPHERIC OUTGOING LONG-WAVE FLUX (F_0)
vs. TOTAL NET RADIATIVE COOLING (ΔE_T),
12-16 MARCH 1957, OMAHA, NEBRASKA
[Entries are in $\text{cal cm}^{-2} (3 \text{ hr})^{-1}$]

Date	1500 CST			2100 CST		
	Sky	F_0	ΔE_T	Sky	F_0	ΔE_T
12 March	CLEAR	67	3.5	CLEAR (.1 CLD)	62	26.0
13 March	OVCST (HIGH)	34	-11.5	OVCST	35	30.0
14 March	OVCST + PRECIP.	43	0.0	OVCST + PRECIP	42	34.5
15 March	CLEAR (DRY)	55	9.0	CLEAR	57	32.0

B. Average Energy Loss vs. Energy Loss for Average Conditions

Since studies of the heat budget of the atmosphere usually involve extended periods of time and sizable surface areas, it is frequently necessary to deal with average radiative conditions. In computational studies it is convenient to approximate the average radiative cooling by first describing the average distribution of meteorological variables, and then calculating the radiative cooling for the average conditions. The case study for Omaha provided an opportunity to compare the average of computations of "instantaneous" radiative cooling with the computations of radiative cooling for the average distributions of temperature, moisture, and cloudiness over the entire 3-1/2-day period. This test also corresponds to a comparison of the average of radiative computations at many localities on a fixed latitude with the radiative computations based on the average meteorological conditions for all localities.

With the mean profiles of temperature and mixing ratio for the entire period, the net long-wave flux divergence (cooling) and the net rate of solar absorption (heating) in the troposphere were first obtained for clear skies. Four cloud models were selected to represent the cloudiness during the period. Each cloud type was treated as an overcast occurring with the mean temperature and moisture distributions. Calculations for each sky condition were weighted by that fraction of the total time period represented by the sky condition. Of the four model clouds, only two occurred during the daylight hours. All of the calculations of solar absorption (for the mean moisture distribution) were based on a mean zenith angle for the day. The reflectivity and absorptivity of daytime clouds were adopted from an earlier study.¹⁰

In addition to the calculations with four cloud types, both the long-wave cooling and short-wave heating were determined for average conditions by a hypothetical single-cloud representation of average cloudiness (i.e., an effective cloud with average base and top heights). Results for the single effective cloud were not significantly different in this case from the more lengthy treatment of four cloud types. The technique of using "average" clouds might best be improved by adopting two effective clouds, one for night and one for day.

Table II summarizes the comparison of the actual average tropospheric radiative cooling and the radiative cooling deduced from the average meteorological conditions (using four cloud types). The outstanding feature of the computations based on the mean meteorological conditions is that they significantly overestimate the actual average rate of loss of energy. The overestimate results from an exaggerated long-wave cooling in conjunction with a more serious underestimate of the solar heating. The bias is increased by the weighted inclusion of clouds. Barring errors in computation, the bias must result from improper representation of average conditions and actual differences between the average radiative cooling and the radiative cooling for average conditions. A high degree of reliability cannot be placed on the absolute magnitudes appearing in Table II, but relative differences should be realistic.

Table II

ACTUAL AND ESTIMATED AVERAGE RADIATIVE COOLING RATES IN TROPOSPHERE

12-16 MARCH 1957, OMAHA, NEBRASKA

[Entries are in cal cm⁻² (3 hr)⁻¹]

	Actual	Estimated from Mean Data				Mean State
		Clear	Cloud I	Cloud II	Cloud III	Cloud IV
Long-Wave	27.8	28.9	17.0	24.0	32.1	41.8
Solar*	-10.1	-5.9	-3.5	--	--	-6.2
Total Net Cooling	17.1					31.0
						-5.4
						25.6

* Tabulated averages include zero heating for nocturnal hours.

Cloud I: top, 350 mb; base, 500 mb

Cloud II: top, 350 mb; base, 700 mb

Cloud III: top, 700 mb; base, 950 mb (Precip.)

Cloud IV: top, 500 mb; base, 950 mb (Precip.)

The large underestimate of the average solar heating rate arose from the adoption of a single mean zenith angle for computations of the average day. Ideally, a zenith angle should be selected so that the corresponding solar heating rate agrees with the average daily heating rate. However, even for a given latitude and season, it is difficult to describe uniquely a representative zenith angle for all conditions. Obviously, the mean zenith angle adopted should have been smaller. The most appropriate single angle appears to be largest for clear and dry conditions and smallest for cloudy conditions. Consequently, estimates of the average solar heating rate from mean conditions might best be obtained by the more lengthy procedure of first computing absorption rates at a number of equally spaced times during the half-day, and then averaging.

The overestimate of the long-wave cooling is most probably related to the radiative properties of the mean meteorological conditions and the manner in which clouds are included. In part, the bias may be due to a more rapid decrease in moisture above the clouds in the mean sounding than in the actual soundings associated with the clouds. Without a more extensive study of a number of additional cases, it is premature to state definitively the size of the bias that is likely to result by estimating the average radiative cooling from computations with averaged meteorological data. The Omaha conditions may have represented an extreme, so that the addition of several days could have reduced the bias.

REFERENCES

1. P. M. Furukawa and W. Viezee, "An Analysis of the Outgoing Infrared Radiation at Omaha, Nebraska, 12-16 March 1957," Scientific Report 1, Contract AF 19(628)-322, Stanford Research Institute, Menlo Park, California (1962).
2. D. Q. Wark, "Applications to Radiation Processes in the Atmosphere," Abstracts and Figures of Lectures, The International Meteorological Workshop, Washington, D.C. (1961).
3. S. Fritz and J. S. Winston, "Synoptic Use of Radiation Measurements from Satellite Tiros II," Mon. Wea. Rev. 90, 1, pp. 1-9 (1962).
4. W. R. Bandeen, R. A. Hanel, John Licht, R. A. Stampfl, and W. G. Stroud, "Infrared and Reflected Solar Radiation Measurements from Tiros II Meteorological Satellite," J. Geo. Res. 66, 10, pp. 3169-3185 (1961). Also see NASA Technical Note D - 1096 (1961).
5. R. A. Hanel and W. G. Stroud, "The Tiros II Radiation Experiment," Tellus, 13, 4, pp. 486-488 (1961). Also see NASA Technical Note D - 1152 (1961).
6. W. Nordberg, W. R. Bandeen, B. J. Conrath, V. Kunde, and I. Persano, "Preliminary Results of Radiation Measurements from the Tiros III Meteorological Satellite," J. Atmos. Sci., 19, 1, pp. 20-29 (1962).
7. J. N. Howard, D. L. Burch, and D. Williams, "Near-Infrared Transmission Through Synthetic Atmospheres," Geophysical Research Papers 40, AFCRC, Bedford, Massachusetts (1955).
8. W. M. Elsasser, "Atmospheric Radiation Tables," Meteor. Monographs Am. Meteor. Soc. 4, 23 (1960).
9. K. L. Coulson and P. M. Furukawa, "Distribution of Atmospheric Radiative Heating and Cooling," Scientific Report 2, Contract AF 19(604)-5965, Stanford Research Institute, Menlo Park, California (1960).
10. W. Viezee, unpublished report.

STANFORD
RESEARCH
INSTITUTE

MENLO PARK
CALIFORNIA

Regional Offices and Laboratories

Southern California Laboratories
820 Mission Street
South Pasadena, California

Washington Office
808 17th Street, N.W.
Washington 5, D.C.

New York Office
270 Park Avenue, Room 1770
New York 17, New York

Detroit Office
The Stevens Building
1025 East Maple Road
Birmingham, Michigan

European Office
Pelikanstrasse 37
Zurich 1, Switzerland

Japan Office
911 Iino Building
22, 2-chome, Uchisaiwai-cho, Chiyoda-ku
Tokyo, Japan

Representatives

Honolulu, Hawaii
Finance Factors Building
195 South King Street
Honolulu, Hawaii

London, England
19 Upper Brook Street
London, W. 1, England

Milan, Italy
Via Macedonio Melloni 40
Milano, Italy

London, Ontario, Canada
P.O. Box 782
London, Ontario, Canada